Discrimination between nanocurcumin and free curcumin using graphene quantum dots as a selective fluorescence probe

Esther Pinilla-Peñalver[a,b], M. *Laura Soriano*[a], *Ana M. Contento*[b] *and Ángel Ríos*[a,b,*]

[a] Regional Institute for Applied Chemistry Research (IRICA), 13071 Ciudad Real, Spain.

[b] Department of Analytical Chemistry and Food Technology, Faculty of Chemical Sciences and Technologies. University of Castilla-La Mancha, 13071 Ciudad Real, Spain.

[*] Corresponding author: Prof. Dr. Ángel Ríos. Phone.: +34926295232; E-mail address: Angel.Rios@uclm.es
Orcid: http://orcid.org/0000-0003-1728-3097.

Acknowledgments

This research was funded by Spanish Ministry of Economy and Competitiveness (MINECO) and the Regional Government of Castilla-La Mancha (JCCM) with Grants CTQ2016-78793-P and SBPLY/17/180501/000262, respectively. E. Pinilla-Peñalver also acknowledges MINECO for the predoctoral contract BES-2017-080357. M. L. Soriano expresses her gratitude to the European Commission and the JCCM for the funding project SBPLY/17/180501/000333. We also want to thank M. A. Arranz for the AFM measurements.

Abstract

Accurate-controlled sized graphene quantum dots (GQDs) have been used as a sensing probe for detecting curcumin as function of the photoluminescent quenching upon increasing concentrations of the analyte. Regarding the importance of curcumin nanoparticles in nutraceutical food, the analytical method described herein was also proven for the discrimination of curcumin remaining in free solution from that encapsulated into water-soluble nanomicelles of ca. 11 nm. This recognition is based on the displacement of GQD emission when interacting with both curcumin species. Maximum emission wavelength of GQDs suffers a gradual quenching as well as a red shifting upon increasing concentrations of free curcumin (from 460 to 490 nm, exciting at 356 nm). On the other hand, in presence of nanocurcumin, the GQD photoluminescent response only displays a quenching effect (356/460 nm). The sensitivity of the described method in terms of detection limits were of 0.3 and 0.1 μg mL^{-1} for curcumin and nanocurcumin, respectively. The applicability of the sensing probe for the quantification and discrimination between both curcumin environments was demonstrated in nutraceutical formulations namely functional food capsules and fortified beverages such as ginger tea.

Keywords: sensing method, recognition, red-shifting, bioactive encapsulation, curcuma, nutraceuticals, nanomaterials.

Introduction

The exponential growth of nanotechnology is the result of an outstanding benefits from ever-increasing number of nanomaterials and nanoprocesses in a wide range of fields. For instance, novel engineered nanoparticles (NPs) are constantly reported to be used in medical sciences in several ways like bioimaging or sensing, in electronic or as fluorescence probes to develop new analytical methods. But, at the same time, it is not acceptable the use of these nanomaterials without a complete toxicological information which also involves potential risks for environment and human health. Hence, it is important to develop reliable analytical methods for the control of such NPs, which is a field still relatively unfinished due to the huge variety of them. So far, the use of NPs for analytical purposes presents three points of view. In the first, the NPs are used as a tool to develop analytical methodologies, especially involved in the preparation of samples and in the detection step of the analytical process. In the second form, nanomaterials are considered as target analytes in specific samples, and the last point of view is the determination of nanomaterials using another one as analytical tool **[1, 2]**. This approach is exploited in this work, where we have selected a widely used nanomaterials for food nanotechnology and for medical purposes in recent years, nanosized formulation of curcumin (curcumin nanomicelles). GQDs are used as analytical tool for the determination of nanocurcumin.

Curcuminoids belongs to the *Curcuma longa L*. family with substantial health benefits, namely for preventing inflammatory, fungal microbial and oxidant activities and for its antiproliferative features and low toxicity. The major curcuminoid found in food as bioactive substance (as colouring, flavouring and spice agents) is the lipophilic curcumin, able to penetrate cell membranes and wield their pharmacological actions **[3]** (anti-inflammatory, antioxidant, anticancer and antimicrobial effects) and chemoprotective properties (antiproliferative, anti-invasive and antiangiogenic properties) for improve the treatment of several diseases **[4-8]** (Parkinson, Alzheimer, sclerosis, diabetes or arthritis). Other two minor curcuminoids found in commercially available curcumin are demethoxycurcumin (17%) and bisdemethoxycurcumin (3%) **[9]**, which are less active in the treatment of some diseases. All of them are characterized by poor aqueous solubility (~11 ng mL^{-1} for curcumin) and thus a low bioavailability **[10]**, high instability or degradation at basic aqueous medium **[11]** and under light radiation, limiting their distinctive benefits. Food technologies have achieved solutions to such inconveniences by encapsulating curcumin into macromolecules and nanostructures (using cyclodextrin cavities and lipid nanostructures, namely micelles, nanogels or phospholipid complexes as new carrier systems) to improve thus their permeation and penetration into the body **[12, 13]**. Once encapsulated, nanocarrier systems transport the active substance through the

gastrointestinal tract into the bloodstream, achieving greater bioavailability. Encapsulated curcumin is now found in many food and dietary supplements. However, some of these nanoformulations suffered major food-safety considerations **[14]** due to surfactants and other stabilizing additives for preventing agglomeration and speeding the encapsulation of the active ingredients. Thus, these nanotechnological approaches as outstanding solutions may have a negative connotation as occurred with engineered NPs **[15]**. Furthermore, few toxicological information about these nanosized formulations of curcumin is evaluated. Thus, is important to pay more attention to monitor and quantify the fabrication and stabilization of such nanosized curcumin in food and supplementary matrices as well as inside the human organs. Only a few works reported the determination of different curcumin formulations by fluorometric **[16]** or HPLC methods **[17-20]**, but those methods always involved the breakup of the curcumin-containing nanosystems to detect and quantify curcumin in free solution (refereed as Cur).

Thus, the monitoring of diverse curcumin nanosystems prepared by food technology is needed. We focus our attention in detecting a lipid-based nanocarrier, encapsulated curcumin into nanosized micelles (refereed as nanocurcumin, NCur) as one of the most common nanosized formulations in nutraceuticals. In this regard, it is especially important to develop alternative ways to the classical analytical methodologies, such as the use of fluorescent carbonaceous nanomaterials as analytical tools because of the prominent opportunities they offered in a variety of research fields [**2**,**21**].

GQDs are a kind of carbon-based nanodot synthesized in the last decades **[22]** and characterized by their high surface area, low-toxicity, high water solubility, tuneable surface functionalities, and exceptional optical and electrical properties which can be exploited in the development of interesting applications **[23-25]**. The graphitic structure with multiple functionalities at the edges seems to be a good candidate as fluorescent probe for developing real-world analytical tools able to distinguish between diverse food formulations, which it seems to be lacking in literature.

This paper presents for the first time a simple approach based on the use of GQDs as a fluorescence detection strategy, to discriminate between NCur and Cur. This example contributes to the third way of Analytical Nanoscience and Nanotechnology **[26]** that incorporated nanomaterials as tools and analytes, both in the same analytical process. In addition, its applicability as a fluorescence sensor for the recognition of both forms of curcumin in several matrix samples was investigated and reliable results were obtained. The proposed method was also applied for the quantification of NCur and Cur in tea samples and NCur contained in a nutraceutical food.

Experimental

Reagents and materials

All chemical reagents were obtained from commercial sources of analytical grade and were used as received without further purification. Uric acid (UA, ≥ 99.0%) was purchased from Alfa Aesar and sulfuric acid (98%) was acquired from Labkem. Curcumin mixture (≥ 64.0%), analytical standards of curcumin (≥ 98.0%), desmethoxycurcumin (≥ 95.0%) and bisdemethoxycurcumin (≥ 95.0%), sodium hydroxide (98.0%), polyethylene glycol sorbitant mono-oleate (tween 80), 4-morpholineethanesulfonic acid hydrate (MES, ≥ 99.5%) and Kaiser test kit were obtained from Sigma Aldrich (Madrid, Spain). Quinine sulfate dihydrate (≥ 99.0%) was acquired from Acros Organics (New Jersey, USA). Other interference species such as omega-3, glucose, sucrose, lactose, vitamin D, sodium dodecyl sulfate (SDS) and potassium, calcium and sodium chloride were acquired from Sigma Aldrich (Madrid, Spain). All aqueous solutions were prepared using 18.2 MΩ cm water, purified with a Milli-Q water system (Millipore, Molshem, France). Solvents as acetone (≥ 99.9%), methanol (≥ 99.9%), hydrochloric acid (37%) and absolute ethanol (99.8%) were obtained from Panreac (Barcelona, Spain).

Stock standard solution of curcumin was prepared in ethanol at pH 6 fixed with MES hydrate buffer. All solutions were kept at room temperature in absence of light. Regarding the samples, curcumin encapsulated into nanomicelles in the format of capsules were purchased from NovaSOL company (www.cellinnov.com) while ginger tea was acquired from a local supermarket.

GQDs and nanocurcumin were filtrate in nylon membranes for 0.45 μm pore size previously to perform all the measurements.

Instrumentation

Absorption spectra of GQDs and the curcuminoids were obtained using a SECOMAN UVI Light XS 2 spectrophotometer equipped with a LabPower V3 50 using 10 mm quartz cuvettes. Fluorescence spectra were recorded on a QuantaMaster40 spectrofluorometer from Photon Technology International equipped with a 75 W continuous xenon short arc lamp using a detector voltage of 981 V. SOC-10 USB interface FelixGX software was used to collect and process fluorescence data. Emission and excitation slit widths were both 2 nm unless otherwise specified. All optical experiments were performed at room temperature.

144 Infrared spectra of the solid powder of GQDs was recorded with a crystal ATR of ZnSe Shimadzu,
145 IRAffinity-1S model and DTGS Standard detector. Raman measurements of GQDs were performed
146 by a portable Raman spectrometer model B&W TEK (i-RAMAN BWS415) using a 785 nm
147 wavelength laser operating at a maximum output power of 300 mW. The solid sample was deposited
148 on a silica (SiO_2/Si) plate. Exposure time was set at 10,000 ms per scan and GQD Raman curve was
149 the average of 3 scans for a total integration time of 30 s. Acquisition data was obtained with a
150 BWSpec4^{TM} software.

151 Particle size distribution, polydispersivity index and zeta potential of the nanostructures were
152 determined by dynamic light scattering (DLS) measurements using a Zetasizer Nano system (Malvern
153 Instruments Limited, Spain) at 25 ºC using ultrapure water as the dispersing medium.

154 The morphology was studied by atomic force microscope (AFM) using a NT-DMT Solver model.
155 The dispersion of GQDs was diluted (1:5) using ultrapure water into a thin mica plate.

156 The pH of all aqueous solutions used were measured using a Crison Basic 20 pH-meter with a
157 combined glass electrode (Barcelona, Spain). An ultrasonic cleaning bath Ultrasounds (Selecta), a
158 microcentrifuge BioSan Microspin 12 (LabNet Biotecnica S.L.), a vortex stirrer V05 series (LBX
159 instruments) with speed control, and 254/365 nm UV lamp 230 V, E2107 model, Consort nv
160 (Turnhout, Belgium) were also used.

161 **Measurement of quantum yield**

162 The relative quantum yield (QY) was calculated by measuring the fluorescence of GQDs prepared at
163 200 ºC as previously reported **[27]**. It was used quinine sulfate as the fluorophore of known QY Ref
164 QY abajo under the same experimental conditions since it is comparable to the ensuing GQDs. All
165 measurements were carried out in 1 cm quartz cuvettes at room temperature. Absorbance was
166 measured below 0.1 at excitation wavelength of 356 nm in order to reduce readsorption effects.

167 **Preparation of encapsulated curcumin**

168 A curcumin solution (4 mM) in ethanol was added dropwise into 5 mL of aqueous solution of tween
169 80 to achieve a final concentration of 1 mM (> critical micellar concentration, CMC) with 6% of pure
170 curcumin. Nanocurcumin was formed after stirring and sonicating the mixture during 10 and 5
171 minutes, respectively (Fig. 1). The incorporation of the active ingredient into the micellar component
172 was carried out at room temperature. All solutions were kept protected from light. In order to remove
173 the unloaded curcumin into the nanomicelles, curcumin-loaded micelles were filtered in a 0.45 µm
174 pore-size filter membrane, assuming the retained curcumin being outside the micelle (non-

encapsulate). The concentration of nanocurcumin in each filtered solution was then recalculated taking into consideration the quantification of non-encapsulated curcumin (free curcumin) after being eluted from the filter with methanol and measuring the subsequent concentration spectrophotometrically at 425 nm.

The encapsulation efficiency (%EE) of curcumin into tween 80 nanomicelles was determined after the separation of curcumin-loaded nanoparticles, NCur, from non-entrapped curcumin, Cur, using a nylon filter membrane. The entrapment efficiency was calculated as:

$$\%EE = \frac{[Curcumin]_{total} - [Curcumin]_{free}}{[Curcumin]_{total}} \; x \; 100 \qquad (1)$$

For this type of delivery system, the entrapment efficiency of curcumin into the micelles resulted to be 92%.

Samples preparation and analytical procedure

Tea samples were prepared as usual; briefly, a tea bag of ginger was immersed into 30 mL of deionized water (adjusted to pH 6 with 15 mM MES buffer) for 5 minutes at room temperature. The brownish tea solution was filtered in order to remove any suspended tea particle and the filtrate was used to prepare the working solution for the analysis. The samples were enriched at four concentration levels from 2.5 to 20.0 μg mL^{-1} of Cur or between 0.8 and 2.3 μg mL^{-1} of NCur.

For preparation of a commercial nutraceutical food sample namely NovaSOL curcumin, the viscous oil content of a capsule of this product was dissolved and stabilized in a mixture of 1 mM of tween and 15 mM MES buffer at pH 6. The resulting solution was filtered in a 0.45 μm nylon membrane for the estimation of the concentration of NCur in the sample.

In the interaction studies, GQD aqueous solutions (200 μL, 16 μg mL^{-1}) were mixed with curcumin solutions (200 μL of free or nanoencapsulated one) at pH 6 at room temperature for 5 min under stirring to ensure complete interaction. After that, these mixtures were transferred into a 10 mm quartz cuvette to perform the optical measurements avoiding the incidence of light.
Fluorescence measurements were carried out recording the emission spectra of GQDs between 376 and 600 nm using an excitation wavelength of 356 nm. Both excitation and emission slit widths were set at 0.5, while the step size and integration time were of 2 nm and 0.3 seconds, respectively. The I_0/I ratio was used as analytical signal, where I_0 and I were the maximum fluorescence emission intensity of GQDs in absence and presence of curcumin species, respectively. When samples were

analysed, Cur or NCur standard solution were replaced by the nutraceutical food or tea samples prepared as described at the beginning of this section.

Discrimination between free curcumin and nanocurcumin was performed by monitoring the red shifting in the emission wavelength of GQDs.

Results and discussion

Characterization of GQDs

Fluorescent graphitic structures have been synthesized following the bottom-up approach previously described by us **[27]**. Carbonization of uric acid at diverse temperatures were studied. In the synthetic conditions, the heating process was crucial to achieve GQDs of high quality. At temperatures of 180 ºC, the resulting solution displayed a high photoluminescent properties although the emission was excitation dependence as a result of the multiple emitters presence, as occur in other carbon nanodots **[28]**. However, at 200 ºC a more controlled process for the bottom-up fabrication of pure graphene nanolayers were obtained since the emission was not tunable with the excitation wavelength.

The GQDs average size found by DLS (n=3) under the appropriate conditions (6.4±1.4 nm, see Fig. S1) is consistent to the 6±0.8 nm circular flat sheets that were observed by AFM measurements (n=3) (Fig. S2).

Optical properties of GQDs are of great importance. Fig. S3 shows the yellow aqueous solutions of the nanodots at diverse pH values under sunlight and displaying different blue fluorescence intensities under the UV-light irradiating at 365 nm. Fig. S3C illustrates differences in the GQD fluorescence according to the pH value, showing the maximum fluorescence at pH 7.5. GQD absorption (blue line), excitation (green line) and emission (orange line) spectra show characteristic profiles consistent to previous studies **[27]**, as can be observed in Fig. S4. Thus, GQDs exhibit sharp absorption peaks at 222 and 262 nm characteristic to the π-π* transitions of sp^2 carbon hybridization and a broader absorption band at 375 nm, attributed to the n-π* transitions by the presence of C=O as surface defects in the graphene layer.

Besides, the maximum excitation wavelength differs depending on pH**,** suggesting the presence of ionisable groups at the graphitic edges. GQD emission band at 460 nm when exciting at the maximum wavelength (λ_{exc} 356 nm) displays a full width at half maximum of 81 nm, indicating a narrow size distribution of the nanolayers. On the contrary of their analogues carbon quantum dots and carbon nanodots **[21]**, the GQD emission found is not tunable as a result of the maximum emission wavelength being independent on the excitation, implying uniformity in both size and surface states

of the ensuing graphitic layers. That fact suggests that the individual emitters within the nanolayer lack of a collective effect from diverse compositions of particle surfaces-cores. Regarding the probability of the excited sate being deactivate by fluorescence, QY of GQD aqueous solution resulted to be 0.41 using quinine sulfate (dissolved in 1N H_2SO_4, QY 0.54) as reference **[29]**, being this value similar to that obtained in previous publications **[27]**.

Interestingly, it was found that the emission intensity of the nanodots remain unchanged in presence of ethanol, while the signal stability fluctuates in presence of different proportions of methanol.

Raman profile of GQDs (Fig. S5a) shows the characteristic bands of graphitic structures at 1309 (D band) and 1593 cm^{-1} (G band). At around 2615 cm^{-1} the 2D band is also observed. I_D/I_G ratio for the ensuing GQDs resulted to be of 1.18, indicating the presence of abundant defects in the structure. In solid state, IR characteristic peaks of GQDs (Fig. S5b) at 3150 and 3062 cm^{-1} suggests the presence of N-H stretching vibrational modes of amide functionalities possibly forming hydrogen bonding **[30]**. Bands at 2830 and 612 cm^{-1} are related to aliphatic CH stretching and deformation vibrations attributed to the aromatic framework containing any alkane fragments, respectively. Other peaks at 1688, 1580, 1408 cm^{-1} may be associated to C=O, C=C, C-O-H stretching vibrational modes of the aromatic framework. Interestingly, Kaiser test results corroborated the presence of free amine groups; the average content, measured in quintuplicate, resulted to be in 13.8±1.5 μmol g^{-1} at the graphitic nanolayer (Table S1).

Preparation and characterization of free and encapsulated curcumin

Nanoparticle-based delivery systems are widely used to produce nutraceuticals of several active ingredients **[31]**. In this work, non-ionic surfactant tween 80, which is safely used in food, was selected giving rise to clear solutions of micelles of small sizes with excellent thermodynamically stability and easy encapsulation features. Due to the low water solubility of curcumin, it is convenient the use of a small percentage of organic solvent, being ethanol chosen for producing lees toxic and more stable solutions. In addition, to avoid curcumin degradation into vanillin, *p*-hydroxybenzaldehyde, ferulic aldehyde, *p*-hydroxybenzoic acid, vanillin acid and ferulic acid, standard curcumin solutions were prepared fresh daily and protected from light.

In order to obtain curcumin-loaded nanoparticles with satisfying properties, several processing parameters were investigated including type of solvent, pH of the medium, type and concentration of the buffer, surfactant and curcumin concentrations, stirring and sonication time. The best conditions to obtain NCur were using ethanolic Cur solution at 4 mM. Such Cur solution was added dropwise to an aqueous phase containing 1.15 mM of empty nanomicelles from tween 80, formed by exceeding its CMC. Considering the pH range to avoid the micelle breakage, the selected pH of the micellar

solution was fixed at 6 with MES hydrate buffer. Nanomicellar curcumin was prepared employing 90.7% of tween 80 with a final concentration of 1 mM and 9.3% of curcumin powder (6% pure curcumin). These proportions vary according on the purity of the bioactive. Both phases then homogenised with high stirring in vortex for 10 minutes and then another 5 minutes of sonication to facilitate the penetration of the active ingredient into the micelles. After that, filtration took place in a 0.45 μm nylon filter to separate the NCur formed from the remaining non-encapsulated curcumin, Cur, which was retained in the filter membrane. The hydrophobic force of Cur driven aggregation, enabling its retention in the filter. Previously, it was verified that Cur contained in ethanolic solution was completely retained in a nylon filter membrane whilst NCur passed through it. The separation of Cur from NCur was corroborated using spectrophotometry and DLS techniques.

The optical and microscopic characterization of synthesised NCur was carried out. Fig. 2a shows the absorption spectra of NCur and ethanolic solution of Cur. As can be seen, absorption of Cur resulted in a small band at 265 nm and a main band centered at 425 nm, attributed to n-π* and π-π* transitions, respectively **[32]**. However, NCur displays a narrower band slightly shifted to 420 nm with a small shoulder at 445 nm **[33]**. This confirms that the encapsulation of curcumin did not affect its chemical properties. By examining the fluorescence properties of both species (Fig. 2b), it is evidenced the encapsulation process, since a blue shift in the emission of NCur with respect to Cur was found. Thus, the blue shifting in the absorbance and fluorescence spectra of NCur are likely due to the intermolecular interactions between the bioactive and hydrophobic inner shell of tween 80.

The surface charge, hydrodynamic size and size distribution of the ensuing nanomicelles were measured by DLS technique. The zeta potential value of NCur resulted to be -15.1±3.4 mV, indicating that these NPs are stable in solution. Fig. 3a shows the narrow size distribution and average diameters of empty and filled micelles of 8.7±1.3 nm and 10.9±1.9 nm, respectively. As expected, the size of the empty nanomicelles was smaller than the loaded one with curcumin. SEM analysis (Fig. 3b) provide the spherical morphology of the micelles corroborating the average size of NCur previously obtained by DLS.

To characterize the entrapment efficiency, the amount of curcumin loaded into the tween micelles was established as the difference between the total concentration used to prepare the micellar solution and the curcumin concentration recovered from the filter membrane, free curcumin. To calculate the second concentration, the residue retained in the filter was completely eluted in methanol and redissolved in ethanol and measuring their concentration by spectrophotometry at 425 nm. Thus, a

micellar solution (1 mM tween 80) prepared with 136.9 µg mL^{-1} of curcumin resulted after filtration in a solution of 127.1 µg mL^{-1} loaded into the micelles, being the entrapment efficiency of 92%. Table S2 summarized the physicochemical characteristics of synthetized nanocurcumin which are very appropriate for food industry **[34]**.

Effect of chemical variables in the interaction between free or nanoencapsulated curcumin and graphene quantum dots.

The potential for developing a novel fluorescent probe for the discrimination between free and nanoencapsulated curcumin based on GQD systems was studied. In this context, several parameters were optimized. Suitable concentration of GQDs was established at 8 mg L^{-1} since the maximum ratio of intensities (I_0/I) was observed.

Interaction time was evaluated from a few minutes to weeks. Time-dependence experiments were then carried out to study the stabilization time of GQDs-Cur and GQDs-NCur systems. Only 30 seconds under continuous stirring and 5 minutes of reaction were enough to achieve a stable fluorescence signal.

The influence of pH on the system was a critical parameter to optimize owing to the low stability of curcumin at extremely acidic pH due to its presence in the protonated form and at pH above 7. The high stability of curcumin in slightly acidic medium is attributed to the conjugated diene structure, which under neutral or basic conditions is destroyed when the phenolic OH is deprotonated **[35]**. On the one hand, preliminary experiments visually corroborate such evidences as curcumin solutions remained bright yellow at pH values between 4 and 7.5 and turned into orange-red colour at pH values higher than 7.5. In addition, according the manufacturer information, pH values higher than 8 changes the stability of the micelles. On the other hand, it was shown that maximum fluorescence emission for GQDs occurs at pH values between 5 and 12. Taking into account all the above considerations, the pH effect among 5 and 7.5 on the free and encapsulated curcumin interaction with GQDs was studied by measurements of fluorescence intensity in the absence (I_0) and in presence (I) of curcumin species. The maximum emission value was obtained for pH 6, fixed with MES hydrate buffer solution in both systems, further providing greater stability to interaction system. Therefore, this pH value was selected for the following experiments. Moreover, the effect of the ionic strength on I_0/I signal ratio of GQDs was also investigated. This experiment was carried out using MES buffer solutions (pH = 6) in the 3.2-30.0 mM concentration range. The results showed that the higher fluorescence quenching and emission shifting was obtained at 15 mM concentration of MES buffer.

Given the low solubility of curcumin in aqueous solutions, another parameter examined was the minimum alcohol content necessary to keep curcumin solutions stable. Therefore, the variation of

ethanol studied was in the range of 25-65%. Thus, higher interaction between both curcumin species and GQDs resulted at solutions containing 50% of ethanol.

In addition, the fluorescence signal was examined inter-day remaining constant after 7 days; after that, it was progressively decreased.

Discrimination between free and encapsulated curcumin for its interaction with graphene quantum dots

To study the feasibility of the detection system based on GQDs as fluorescence probe, emission spectra of GQDs in absence and presence of free and nanosized curcumin were recorded. It was observed that GQD emission suffered a progressive quenching effect as function of increasing curcumin concentrations either in presence of free or nanoencapsulated media, as shown in Fig. 4. However, despite a similar quenching effect observed for both types of curcumin species, a clear difference exists between both systems. A significant red shifting in the maximum emission wavelength of GQDs when interacting with free curcumin (Fig. 4a) was observed, however there is no shift in the maximum GQD emission when interacting with nanocurcumin (Fig. 4b).

These facts let us detect curcumin and discern in which media is dispersed by monitoring the maximum emission wavelength of GQDs in presence of curcumin species, which remained constant at 460 nm in presence of NCur, and red-shifted as concentration of Cur increases.

To verify that this effect is only due to the presence of curcumin in different media, several preliminary experiments demonstrated that GQD fluorescence did not undergo any alteration in presence of empty micelles (Fig. S6). This result suggests that the nanodots do not penetrate into the micelles. Then, we can ensure that composition of nanosized formulation is not responsible of these effects and GQDs fluorescence is selective to free and encapsulated curcumin formulations.

Sensing mechanisms

Similar quenching behaviour in the interaction of GQDs-Cur or GQDs-NCur was found although a red-shifting on the emission response is produced only for GQDs-Cur system. This fact means that graphitic layers containing functionalities may interact distinctively with both analyte environments. The most probable interaction takes place between nitrogen and oxygen-containing groups of GQDs and the keto-enol bridge (acting as donor and acceptor of hydrogen bonds in its open conformation due to the polarity in which is found) of curcumin producing an effective reduction of GQD fluorescence in both cases. In curcumin, as the keto-enol bridge saturates its donor or acceptor activity of hydrogen bonding, the hydroxyl groups of the phenolic rings become important in the interaction with GQDs. We expected that π-stacking interactions may reinforce the hydrogen bonding previously

mentioned (Fig. S7). It seems that π-stacking interaction plays an important role in the red-shifting of GQD fluorescence in presence of Cur whilst such interaction did not occur in GQD-NCur system.

Analytical features for the determination of free curcumin and nanocurcumin

Several analytical performance features were evaluated in order to examine the possible applicability of GQDs either free or encapsulated curcumin into nanomicelles, as fluorescent recognizing systems. Thus, a linear response was assessed by representing the analytical signal −*relative fluoresce response* I_0/I *(exciting at 356 nm)*− versus increasing concentrations of Cur and NCur under the optimized experimental conditions. Fluorescence intensities (I) of GQDs in presence of different concentrations of NCur were selected at the emission wavelength of 460 nm whilst the GQDs-Cur intensities were recorded at the maximum emission wavelength of the system. The quenching efficiencies followed the Stern-Volmer equation obtaining good relationships with determination coefficients higher than 0.997 in the 1-25 and 0.3-4.5 μg mL^{-1} ranges for Cur and NCur systems, respectively.

The precision was evaluated in terms of repeatability and reproducibility expressed as relative standard deviation (RSD). To determine the repeatability, ten analyses of samples containing 9 μg mL^{-1} of free curcumin or 2 μg mL^{-1} of nanocurcumin were carried out and RSD values of 4.0 and 3.8% were obtained, respectively. Reproducibility was assessed by triplicate at same curcumin concentrations under inter-day conditions (for three consecutive days), obtaining RSD of 5.3 for Cur and 5.0 for NCur.

The sensitivity of the proposed method was evaluated in terms of detection (LOD) and quantification (LOQ) limits, which were established as three or ten times the standard deviation of the blank signal divided by the calibration curve slope, respectively. Interestingly, higher sensitivity resulted to be for the encapsulated curcumin since the calculated LOD values were of 0.3 and 0.1 μg mL^{-1} for Cur and NCur, respectively.

The analytical figures of merit for both systems are summarized in Table 1. These results demonstrated the great potential of GQDs as sensing tools for monitoring free and nanoencapsulated curcumin in different environments.

Interference study

To evaluate the selectivity of the proposed analytical methodology, interference studies were carried out using both types of curcumin species to investigate the effects of possible species present in nutraceutical formulations and other samples of our interest.

The study was performed by adding different amounts of the possible interfering compound to a solution containing GQDs and 2 and 9 μg mL^{-1} of encapsulated or free curcumin, respectively. Possible interfering compounds of food, beverages and nutraceutical formulations, specially quinolone, magnesium stearate and titanium oxide, were eliminated by filtration of the samples. Other substances such as omega-3, glucose, sucrose, lactose, vitamin D and SDS and cations as K^+, Ca^{2+} and Na^+ did not affect the analytical signal even at high concentration levels. In addition, curcuminoids namely bisdemethoxycurcumin and demethoxycurcumin, were also evaluated, being both studied when free and encapsulated into nanomicelles at two concentrations levels (at 27 and 45 μg mL^{-1} for the free curcuminoids and at 6 and 10 μg mL^{-1} for nanocurcuminoids). These curcuminoids produced a similar GQD emission behaviour. Since these curcuminoids are mixed with curcumin in very low proportions **[9]**, the emission effects resulted to be negligible.

Analytical applications

In order to demonstrate the potential applicability of the proposed analytical method, ginger tea samples were fortified at four concentration levels of Cur or NCur. These samples were prepared and submitted to the analytical procedure described in "*Samples treatment and analytical procedure*" section. The matrix effect was previously evaluated to consider the possible interferences that can be exist, observing no effect on the GQDs emission due to the tea matrix. Through DSL analysis, it was found that NCur particle size was not modified when it was added to tea samples.

Fig. 5 shows the behaviour in the fluorescence intensity of GQDs in presence of tea samples spiked with Cur or NCur. It is observed a quenching effect in both cases and a significant shifting in the maximum emission wavelength of GQDs when interacting with Cur.

Table 2 depicts the recoveries found for both curcumin species in the tea beverages analysed by triplicate which ranged from 97.7 and 103.0%. These results indicate a good agreement between amount added and those found in both cases.

Furthermore, the proposed analytical method was applied to analysis of NovaSOL-curcumin capsules, a nutraceutical formulation where the manufacturer declare that contain curcumin more bioavailable than standard curcumin extracts. This effect is attributed to a micellar medium in which this compound is found, where curcumin is stabilized and solubilized in an aqueous medium **[13]**.

To determine NCur in this nanoformulated product, preliminary experiments suggested that pH values around 5 to 7 were necessary to maintain the same manufacturing conditions and avoid

micellar destabilization of the bioactive in an aqueous medium. By DLS it was found that the proposed treatment of the sample did not significantly change the size of the nanoparticle.

Fig. 6 shows the suitable functioning of GQDs as nanocurcumin fluorescent sensor in a real sample. This commercial product was analysed by triplicate, according the procedure described in "*Samples treatment and analytical procedure*" section. To evaluate the matrix effect, the determination of NCur was also carried out by standard addition method. The obtained results were 23.3±2.1 g Kg^{-1} (n=3) and 26.2±3.1 g Kg^{-1} (n=3) with and without standard addition, respectively, corresponding to the concentration of NCur found in the NovaSOL sample. The application of student test for a confidence level of 95% demonstrated the statistical coincidence between the concentrations found by the proposed procedure with those obtained by the standard addition method.

Conclusions

A new analytical methodology based on GQDs as a selective fluorescence probe is aimed at detecting, quantifing and tdiscriminating between free and encapsulated curcumin. It was therefore necessary to synthesize curcumin nanomicelles using food technology as one of the most common nanometric size formulations used in food additives and nutraceuticals. The recognition of the selected nitrogen-containing GQDs with both types of curcumin environments is based on the existence of hydrogen bonds and pi-stacking interactions which were easily monitored by recording the emission behaviour. An extra separation step is required for the quantification of both Cu and NCur although it is accomplished by simply filtration the sample in nylon membranes prior analyses. Results demonstrated the suitability of GQDs as a suitable analytical nanotool for distinguishing between diverse food formulations in a real-world challenge, which it seems to be lacking in literature. This approach opens new paths in the analysis of the nanoworld, belonging to the Third way of analytical Nanoscience and Nanotechnology **[26]**.

Compliance with ethical standards

Authors declare that they have no competing interests.

References

1. López-Lorente AI, Valcárcel M (2016) The third way in analytical nanoscience and nanotechnology: Involvement of nanotools and nanoanalytes in the same analytical process. Trends Analyt Chem 75:1-9. https://doi.org/10.1016/j.trac.2015.06.011

2. Cayuela A, Benítez-Martínez S, Soriano ML (2016) Carbon nanotools as sorbents and sensors of nanosized objects: the third way of analytical nanoscience and nanotechnology. Trends Analyt Chem 84:172-180. https://doi.org/10.1016/j.trac.2016.02.016

3. Maheshwari RK, Singh AK, Gaddipati J, Srimal RC (2006) Multiple biological activities of curcumin: a short review. Life Sci J 78(18):2081-2087. https://doi.org/10.1016/j.lfs.2005.12.007

4. Park EJ, Jeon CH, Ko G, Kim J, Sohn DH (2000) Protective effect of curcumin in rat liver injury induced by carbon tetrachloride. J Pharm Pharmacol 52(4):437-440. https://doi.org/10.1211/0022357001774048

5. Miller E, Markiewicz L, Kabzinski J, Odrobina D, Majsterek I (2017) Potential of redox therapies in neurodegenerative disorders. Front Biosci 9:214-234. https://doi.org/10.2741/e797

6. Lee WH, Loo CY, Bebawy M, Luk F, Mason RS, Rohanizadeh R (2013) Curcumin and its derivatives: their application in neuropharmacology and neuroscience in the 21st century. Curr Neuropharmacol 11(4):338-378. https://doi.org/10.2174/1570159X11311040002

7. Lee WH, Loo CY, Young PM, Traini D, Mason RS, Rohanizadeh R (2014) Recent advances in curcumin nanoformulation for cancer therapy. Expert Opin Drug Deliv 11(8):1183-1201. https://doi.org/10.1517/17425247.2014.916686

8. Miller ED, Dziedzic A, Saluk-Bijak J, Bijak M (2019) A review of various antioxidant compounds and their potential utility as complementary therapy in multiple sclerosis. Nutrients 11(7):1528. https://doi.org/10.3390/nu11071528

9. Sandur SK, Pandey MK, Sung B, Ahn KS, Murakami A, Sethi G, Limtrakul P, Badmaev V, Aggarwal BB (2007) Curcumin, demethoxycurcumin, bisdemethoxycurcumin, tetrahydrocurcumin and turmerones differentially regulate anti-inflammatory and anti-proliferative responses through a ROS-independent mechanism. Carcinogenesis 28(8):1765-1773. https://doi.org/10.1093/carcin/bgm123

10. Siviero A, Gallo E, Maggini V, Gori L, Mugelli A, Firenzuoli F, Vannacci A (2015) Curcumin, a golden spice with a low bioavailability. J Herb Med 5(2):57-70. https://doi.org/10.1016/j.hermed.2015.03.001

11. Kharat M, Du Z, Zhang G, McClements DJ (2017) Physical and chemical stability of curcumin in aqueous solutions and emulsions: Impact of pH, temperature, and molecular environment. J Agric Food Chem 65(8):1525-1532. https://doi.org/10.1021/acs.jafc.6b04815

12. Giri T (2016) Bioavailability enhancement of curcumin nutraceutical through nano-delivery systems. In Grumezescu AM (ed) Nutraceuticals, 1st end. Bucharest, Romania, pp 593-625.
13. Jamwal R (2018) Bioavailable curcumin formulations: A review of pharmacokinetic studies in healthy volunteers. J Integr Med 16(6):367-374. https://doi.org/10.1016/j.joim.2018.07.001
14. Sattigere VD, Ramesh-Kumar P, Prakash V (2018) Science-based regulatory approach for safe nutraceuticals. J Sci Food Agric. https://doi.org/10.1002/jsfa.9381
15. Montes C, Villaseñor MJ, Ríos A (2019) Analytical control of nanodelivery lipid-based systems for encapsulation of nutraceuticals: Achievements and challenges. Trends Food Sci Technol 90:47-62. https://doi.org/10.1016/j.tifs.2019.06.001
16. Mazzarino L, Bellettini IC, Minatti E, Lemos-Senna E (2010) Development and validation of a fluorimetric method to determine curcumin in lipid and polymeric nanocapsule suspensions. Braz J Pharm Sci 46(2):219-226. http://dx.doi.org/10.1590/S1984-82502010000200008
17. Gugulothu DB, Patravale V (2012) A new stability-indicating HPLC method for simultaneous determination of curcumin and celecoxib at single wavelength: an application to nanoparticulate formulation. Pharm Anal Acta 3(4):157. http://doi.org/10.4172/2153-2435.1000157
18. Syed HK, Liew KB, Loh GOK, Peh KK (2015) Stability indicating HPLC–UV method for detection of curcumin in Curcuma longa extract and emulsion formulation. Food Chem 170:321-326. https://doi.org/10.1016/j.foodchem.2014.08.066
19. Ucisik MH, Küpcü S, Schuster B, Sleytr UB (2013) Characterization of curcuemulsomes: Nanoformulation for enhanced solubility anddelivery of curcumin. J Nanobiotechnology 11(1):37. https://doi.org/10.1186/1477-3155-11-37
20. Hasan M, Belhaj N, Benachour H, Barberi-Heyob M, Kahn C, Jabbari E, Linder M, Arab-Tehrany E (2014) Liposome encapsulation of curcumin: physico-chemical characterizations and effects on MCF7 cancer cell proliferation. Int J Pharm 461(1-2):519-528. https://doi.org/10.1016/j.ijpharm.2013.12.007
21. Cayuela A, Soriano M, Carrillo-Carrión C, Valcárcel M (2016) Semiconductor and carbon-based fluorescent nanodots: the need for consistency. Chem Commun 52(7):1311-1326. https://doi.org/10.1039/c5cc07754k.
22. Benítez-Martínez S, Valcárcel M (2015) Graphene quantum dots in analytical science. Trends Analyt Chem 72:93-113. https://doi.org/10.1016/j.trac.2015.03.020
23. Wen J, Xu Y, Li H, Lu A, Sun S (2015) Recent applications of carbon nanomaterials in fluorescence biosensing and bioimaging. Chem Commun 51(57):11346-11358. https://doi.org/10.1039/C5CC02887F

520 24. Durán GM, Contento AM, Ríos A (2015) Sensoring strategies using quantum dots: a critical
521 view. Curr Org Chem 19(12):1134-1149. https://doi.org/10.13140/RG.2.1.1228.1445
522 25. Shen J, Zhu Y, Yang X, Li C (2012) Graphene quantum dots: emergent nanolights for
523 bioimaging, sensors, catalysis and photovoltaic devices. Chem Commun 48(31):3686-3699.
524 https://doi.org/10.1039/c2cc00110a
525 26. Soriano ML, Zougagh M, Valcárcel M, Ríos A (2018) Analytical nanoscience and
526 nanotechnology: where we are and where we are heading. Talanta 177:104-121.
527 https://doi.org/10.1016/j.talanta.2017.09.012
528 27. Durán GM, Benavidez TE, Contento AM, Ríos A, García CD (2017) Analysis of
529 penicillamine using Cu-modified graphene quantum dots synthesized from uric acid as single
530 precursor. J Pharm Anal 7(5):324-331. https://doi.org/10.1016/j.jpha.2017.07.002
531 28. Xia C, Zhu S, Feng T, Yang M, Yang B (2019) Evolution and synthesis of carbon dots: from
532 carbon dots to carbonized polymer dots. Adv Sci 6(23):1901316.
533 https://doi.org/10.1002/advs.201901316
534 29. Melhuish W (1961) Quantum efficiencies of fluorescence of organic substances: effect of
535 solvent and concentration of the fluorescent solute. J Phys Chem 65(2):229-235.
536 https://doi.org/10.1021/j100820a009
537 30. Sharma BK (1981) Spectroscopy. Meerut, Nueva Delhi, India.
538 31. Joye IJ, Davidov-Pardo G, McClements DJ (2014) Nanotechnology for increased
539 micronutrient bioavailability. Trends Food Sci Technol 40(2):168-182.
540 https://doi.org/10.1016/j.tifs.2014.08.006
541 32. Jagannathan R, Abraham PM, Poddar P (2012) Temperature-dependent spectroscopic
542 evidences of curcumin in aqueous medium: a mechanistic study of its solubility and stability. J Phys
543 Chem B 116(50):14533-14540. https://doi.org/10.1021/jp3050516
544 33. Ghosh M, Singh AT, Xu W, Sulchek T, Gordon LI, Ryan R O (2011) Curcumin nanodisks:
545 formulation and characterization. Nanomedicine 7(2):162-167.
546 https://doi.org/10.1016/j.nano.2010.08.002
547 34. Farhang B (2009) Nanotechnology and applications in food safety. In: Barbosa-Cánovas G
548 (ed) Global issues in food science and technology, 1st edn. Pullman, WA, USA, pp 401-410.
549 35. Wang YJ, Pan MH, Cheng AL, Lin LI, Ho YS, Hsieh CY, Lin JK. (1997) Stability of
550 curcumin in buffer solutions and characterization of its degradation products. J Pharm Biomed Anal
551 15(12):1867-1876. https://doi.org/10.1016/S0731-7085(96)02024-9

552

Figure captions

Fig. 1 Illustration of the preparation process of curcumin nanomicelles formulation (b) from free curcumin solution (a)

Fig. 2 Absorbance spectra of Cur, NCur and Tween 80 solutions (a) and the corresponding excitation and emission profiles of Cur and NCur species (b)

Fig. 3 Hydrodinamic sizes of empty and filled nanomicelles measured by DLS technique (a) and SEM micrograph of freeze-dried curcumin-loaded micelles (b)

Fig. 4 Fluorescence emission curves of GQDs in absence and in presence of different concentrations of Cur in the $1 - 35$ μg mL^{-1} range (a) and NCur in the $0.3 - 8$ μg mL^{-1} range (b). Insert: linear relationships between the relative fluorescence intensity ratio and the concentration of curcumin species

Fig. 5 Fluorescence intensities of GQDs in presence of ginger tea samples fortified at different concentrations of Cur (a) and NCur (b).

Fig. 6 Fluorescence emission response of GQDs in the absence and presence of NovaSOL-curcumin commercial formulation containing curcumin-loaded micelles

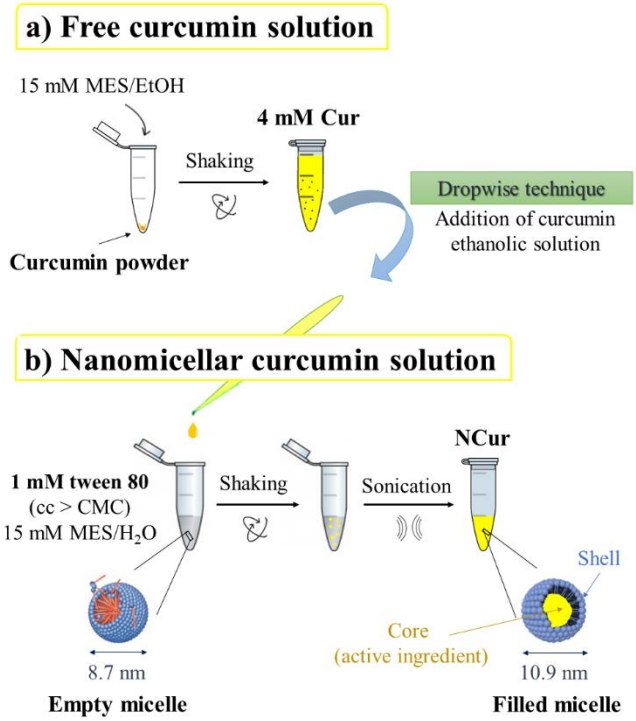
a) Free curcumin solution
15 mM MES/EtOH
4 mM Cur
Shaking
Dropwise technique
Addition of curcumin ethanolic solution
Curcumin powder
b) Nanomicellar curcumin solution
NCur
1 mM tween 80
(cc > CMC)
15 mM MES/H2O
Shaking
Sonication
Shell
Core
(active ingredient)
8.7 nm
10.9 nm
Empty micelle
Filled micelle

Fig. 1

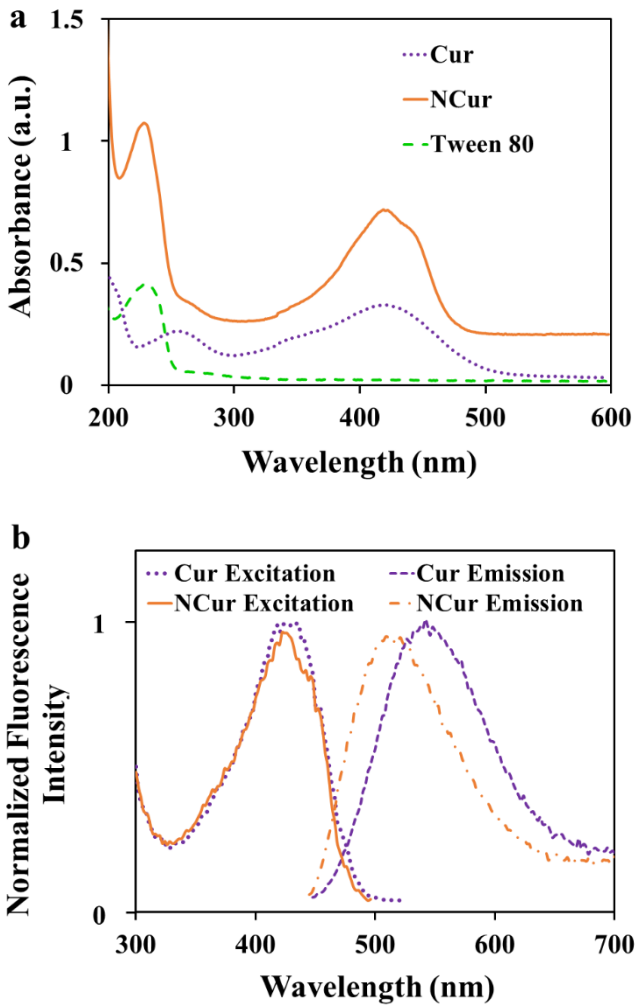
a
1.5
1
0.5
0
Absorbance (a.u.)
Cur
NCur
Tween 80
200
300
400
500
600
Wavelength (nm)
b
Normalized Fluorescence Intensity
Cur Excitation
NCur Excitation
Cur Emission
NCur Emission
1
0
300
400
500
600
700
Wavelength (nm)

Fig. 2

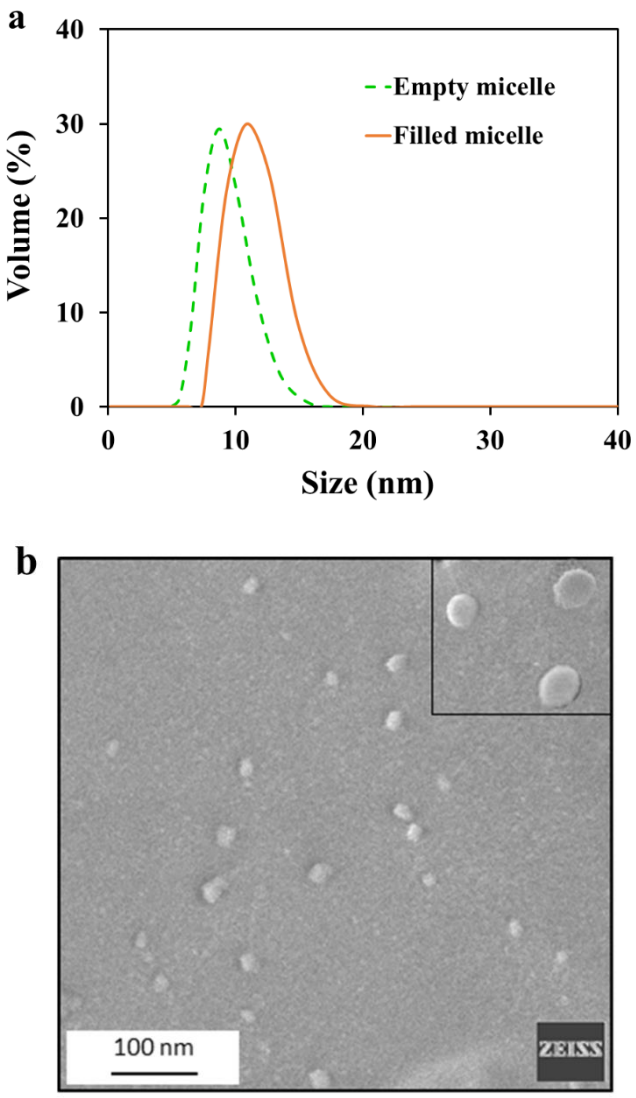
a
40
30
20
10
0
Volume (%)
Empty micelle
Filled micelle
0
10
20
30
40
Size (nm)
b
100 nm
ZEISS

Fig. 3

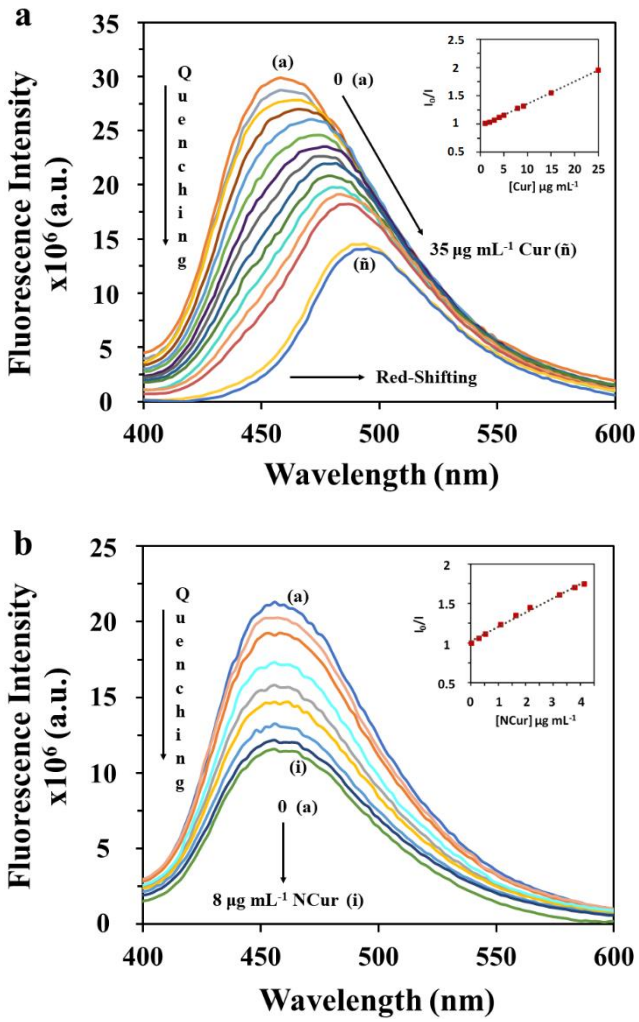
a
Fluorescence Intensity x10⁶ (a.u.)
Wavelength (nm)
Quenching
(a)
0 (a)
35 µg mL⁻¹ Cur (ñ)
(ñ)
Red-Shifting
I₀/I
[Cur] µg mL⁻¹
b
Fluorescence Intensity x10⁶ (a.u.)
Wavelength (nm)
Quenching
(a)
(i)
0 (a)
8 µg mL⁻¹ NCur (i)
I₀/I
[NCur] µg mL⁻¹

Fig. 4

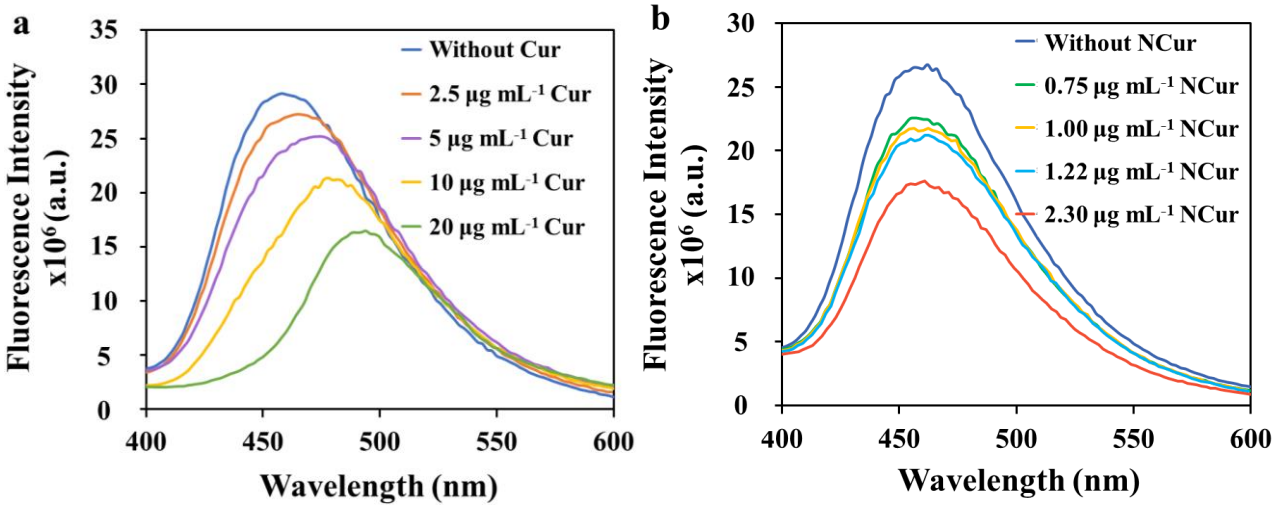
a
Fluorescence Intensity x10⁶ (a.u.)
Wavelength (nm)
Without Cur
2.5 µg mL⁻¹ Cur
5 µg mL⁻¹ Cur
10 µg mL⁻¹ Cur
20 µg mL⁻¹ Cur
b
Fluorescence Intensity x10⁶ (a.u.)
Wavelength (nm)
Without NCur
0.75 µg mL⁻¹ NCur
1.00 µg mL⁻¹ NCur
1.22 µg mL⁻¹ NCur
2.30 µg mL⁻¹ NCur

Fig. 5

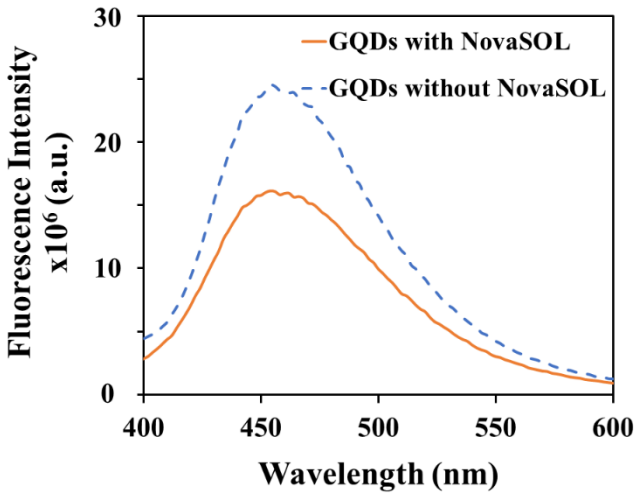
GQDs with NovaSOL
GQDs without NovaSOL
Fluorescence Intensity
x10⁶ (a.u.)
30
20
10
0
400
450
500
550
600
Wavelength (nm)

Table 1. Figures of merit of the proposed method

Parameter	**Free curcumin**		**Nanocurcumin**	
Lineal fit (μg mL^{-1})	$I_0/I=(0.958\pm0.004)+(0.0396\pm0.0009)[Cur]$		$I_0/I=(1.03\pm0.01)+(0.178\pm0.002)[NCur]$	
Linearity range (μg mL^{-1})	1 − 25		0.3 − 4.5	
R^2	0.9993		0.9971	
LOD (μg mL^{-1})	0.3		0.1	
LOQ (μg mL^{-1})	1		0.3	
Repeatibility RSD (%)				
Concentration | I_0/I ratio	4.0	1.8	3.8	0.5
Reproducibility RSD (%)				
Concentration | I_0/I ratio	5.3	2.1	5.0	0.7

Table 2. Recoveries obtained for ginger tea samples spiked with different concentrations of free or encapsulated curcumin

Samples		Concentration added ($\mu g\ mL^{-1}$)	Concentration found* ($\mu g\ mL^{-1}$)	Recovery* (%)
A Ginger tea with Cur	**1**	2.50	2.43±0.03	97.7±1.0
	2	5.00	4.90±0.05	97.9±0.9
	3	10.00	9.83±0.21	98.2±2.1
	4	20.00	20.33±0.46	101.5±2.3
B Ginger tea with NCur	**1**	0.75	0.74±0.006	97.9±0.8
	2	1.00	0.99±0.004	98.2±0.4
	3	1.22	1.20±0.005	98.4±0.4
	4	2.30	2.37±0.013	103.0±0.5

*Analysis performed by triplicate (n=3)